J. Chem. Sci., Vol. 121, No. 3, May 2009, pp. 283–291.

Structural and spectroscopic investigation of lanthanum-substituted strontium-oxybritholites

K BOUGHZALA[1], S NASR[1], E BEN SALEM[1], F KOOLI[2] and K BOUZOUITA[1]*

[1]U.R. Matériaux Inorganiques, Institut Préparatoire aux Etudes d'Ingénieurs, Rue Ibn, ElJazzr, 5019 Monastir, Tunisia

[2]Department of Chemistry, Taibah University, P.O. Box 30002, Almadinah Almunawwarah, Saudi Arabia

e-mail: khaled.bouzouita@ipeim.rnu.tn

MS received 23 July 2008; revised 9 February 2009

Abstract. Lanthanum-substituted strontium-oxybritholites, $Sr_{10-x}La_x(PO_4)_{6-x}(SiO_4)_xO$ with $x = 0$, 2 and 4, prepared by solid state reaction were investigated by chemical analysis, powder X-ray diffraction, Raman and ^{29}Si MAS NMR spectroscopies. The refinements of powder XRD patterns of the substituted compounds by the Rietveld method showed that the lanthanum occupied the two metal sites, i.e. (4f) and (6h) sites into the apatite structure, with a clear preference for the (6h) sites. A progressive shift of the free oxygen O(4) towards the centre of the triangles formed by the metal–atoms in the (6h) positions was observed when the lanthanum content increased. It led to the formation of a Sr/La(2)–O(4) strong bond, which might have increased the stability of these compounds. The bands of Raman spectra were assigned to the vibration modes of PO_4 and SiO_4 groups. The comparison of the results of ^{29}Si MAS NMR analysis with those obtained with the ^{31}P previously reported, suggested that both species occupied the same crystallographic sites.

Keywords. Strontium-oxybritholite; Rietveld refinement; Raman spectroscopy; ^{29}Si MAS NMR spectroscopy.

1. Introduction

Apatites form a large variety of compounds with the general formula $M_{10}(XO_4)_6Y_2$ where M represents a divalent cation (Ca^{2+}, Sr^{2+}, Ba^{2+}, etc.), XO_4 a trivalent anion (PO_4^{3-}, VO_4^{3-}, etc.) and Y a monovalent anion (F^-, Cl^-, OH^-, etc.). They crystallize mainly in the hexagonal system (space group $P6_3/m$).[1–3] A compact arrangement of XO_4 tetrahedrons constitutes the skeleton of this structure which exhibits two kinds of tunnels parallel to the *c*-axis. The first is occupied by four M(1) cations at 4f sites, along a three-fold axis. These cations are coordinated by nine oxygen atoms. The second tunnel which is the larger is occupied, on its periphery, by the six other M(2) cations at 6h sites, along a six-fold axis. These M(2) cations which are surrounded by six oxygen atoms and one Y atom form two alternated equilateral triangles at level 1/4 and 3/4 centred on a six-fold axis where the Y atoms are located. Various cationic,[4–6] anionic,[7,8] or both cationic and anionic[9–12] substitutions may occur in the apatite structure. These substitutions lead to substantial changes in the chemical and physical properties of the obtained materials.

Britholites, rare-earth phosphosilicates, result from the substitution of the divalent cation by a trivalent rare earth element (Ln) and the trivalent XO_4 group by the silicate tetravalent group (SiO_4). This family of compounds attracted researchers' interest because of their potential use as oxide ions conductors[13–15] or confinement matrices for the minor actinides and long-lived fission products.[16,17] However, several studies have shown that the performance of these materials to store nuclear waste decreases with the increase of SiO_4 groups substituting PO_4 ones and the decrease of the fluorine content in the apatite framework.[18–20] In agreement with this, studies focused on the thermodynamic stability of solid solutions $Ca_{10-x}La_x(PO_4)_{6-x}(SiO_4)_xF_2$ and $Ca_{10-x}Nd_x(PO_4)_{6-x}(SiO_4)_xF_2$ where $0 \le x \le 6$ showed that their enthalpy of formation decreased as the substitution of (Ln^{3+}; SiO_4^{4-}) for (Ca^{2+}; PO_4^{3-}) rose,[21,22] while that of their analogue oxybritholites $Ca_{10-x}La_x(PO_4)_{6-x}(SiO_4)_xO$ increased.[23] These two series of compounds differ only according to the

*For correspondence

anion located on the six-fold axis of the large tunnels of the apatite structure. On the other hand, other studies showed that the distribution of lanthanide ions between both cationic sites of the apatite structure is tightly related to the nature of the anion located in these tunnels.[24,25] Moreover, the substitution of silicate groups for phosphate ones has a certain influence on this distribution.[12]

In an attempt to find the structural modifications, an evidence for the opposite evolution of the thermodynamic stability of these two series of compounds when the silicate groups increased in the apatite structure, we decided to undertake the structural refinement of britholites using the Rietveld method in our laboratory.[26] Indeed, only very few structural investigations were performed on these synthetic compounds.[12] In the present work, the results of the structural refinement and spectroscopic studies of lanthanum-substituted strontium-oxybritholites, $Sr_{10-x}La_x(PO_4)_{6-x}(SiO_4)_xO$ with = 0, 2 and 4 are reported.

2. Experimental

2.1 *Synthesis*

Strontium-oxybritholites with the chemical formula of $Sr_{10-x}La_x(PO_4)_{6-x}(SiO_4)_xO$ where $x = 0$, 2 and 4 were prepared by solid state reaction from $SrCO_3$, La_2O_3, SiO_2, $(NH_4)_2HPO_4$ and $Sr_2P_2O_7$.

The strontium diphosphate was prepared according to the following reaction:

$$2SrCO_3 + 2(NH_4)_2HPO_4 \rightarrow Sr_2P_2O_7 + 4NH_3\,(\uparrow) + 2CO_2\,(\uparrow) + 3H_2O\,(\uparrow). \quad (1)$$

A stoichiometric mixture of strontium carbonate and diammonium hydrogenophosphate was ground and homogenized in agate mortar, and pressed into disk. Then, it was calcined in air at 900°C for 10 h.

To achieve (Sr + La)/(P + Si) ratios of 1·67, appropriate reagent amounts were mixed and ground in an agate mortar. The obtained mixtures were uniaxially pressed into pellets of 30 mm in diameter. Then, the samples were calcined under an oxygen flow at 900°C for 12 h with a heating rate of 10°C/min. After cooling to room temperature, the pellets were ground to improve their homogeneity and then pressed again. A second heating process at a temperature ranging between 1200 and 1400°C for 12 h was performed according to the SiO_2 amount. A third heating process was carried out when necessary. The synthesis reaction is:

$$4SrCO_3 + (6-x)/2Sr_2P_2O_7 + xSiO_2 + x/2La_2O_3 \rightarrow Sr_{10-x}La_x(PO_4)_{6-x}(SiO_4)_xO + 4CO_2\,(\uparrow). \quad (2)$$

2.2 *Characterization*

Sr and La contents were determined by inductively-coupled plasma (ICP) using a Shimadzu ICPQ/V-1014S spectrometer. However, Si and P contents were estimated using atomic absorption spectroscopy (Perkin-Elmer 3110) and colorimetrically according to the Gee and Deitz method[27] with a Janway 6400 spectrometer, respectively.

FTIR spectra were recorded with a Perkin Elmer 1283 spectrometer in the range of 1500–350 cm^{-1} using samples pressed into pellets with KBr. Raman spectra were performed at the room temperature in the spectral range of 2000–100 cm^{-1} on InVia Reflex Renishaw Raman microscope equipped with deep-depleted thermoelectrically cooled CCD array detector and a high grade Leica microscope (objective 50×). The spectra were taken using the visible 514·5 nm argon ion laser as the scattering excitation source.

^{29}Si MAS-NMR analysis were conducted at a resonance frequency of 59·62 MHz on a Bruker MSL-300 spectrometer equipped with a cylindrical rotor of zirconium rotating at the frequency of approximately 8 kHz. The reference material for the chemical shift was the tetramethylsilane (TMS).

Powder X-ray diffraction patterns were collected with CuKα radiation using a Philips PW 3070 diffractometer, which was equipped with a diffracted-beam graphite monochromator. The samples were scanned over the 2θ range from 10 to 110° with a step size of 0·02° and a counting time of 12 s per step. Further experimental details of data are listed in table 1. The structural refinement of the three compounds was carried out using the Rietveld method.[28]

3. Results and discussion

3.1 *Chemical analysis*

The results of the chemical analysis of the samples are reported in table 2. The contents of the different elements in the resulting products were close to those expected on the basis of the initial materials that were used. The atomic ratios (Sr + La)/(P + Si) were in agreement with the stoichiometric value of 1·67 for apatites.

Table 1. Unit cell parameters and details of Rietveld refinement of $Sr_{10-x}La_x(PO_4)_{6-x}(SiO_4)_xO$ samples.

Formula	$Sr_{10}(PO_4)_6O$	$Sr_8La_2(PO_4)_4(SiO_4)_2O$	$Sr_6La_4(PO_4)_2(SiO_4)_4O$
Formula weight	1462·026	1558·810	1655·594
Space group symmetry	Hexagonal *P*63/*m*	Hexagonal *P*63/*m*	Hexagonal *P*63/*m*
Formula units per cell *Z*	1	1	1
units cell dimensions			
a (Å)	9·750 (4)	9·756 (6)	9·763(6)
c (Å)	7·278 (3)	7·269 (2)	7·260(2)
units cell volume *V* (Å^3)	599·172(4)	599·168(3)	599·203(5)
Density calculated (g cm^{-3})	4·051	4·319	4·588
Zero point 2θ (°)	0·0707(6)	–0·0384(6)	–0·0552(2)
Number of parameter refined	36	38	38
R_p	6·64	8·04	9·47
R_{wp}	9·10	12·1	13·9
R_B	4·46	4·56	5·79
R_F	3·77	3·58	3·77

Table 2. Chemical analysis of $Sr_{10-x}La_x(PO_4)_{6-x}(SiO_4)_xO$ samples.

Theoretical compositions	Sr	La	P	Si	Sr + La/P + Si
$Sr_{10}(PO_4)_6O$	10·01	–	6·01	–	1·66
$Sr_8La_2(PO_4)_4(SiO_4)_2O$	8·01	1·98	4·00	2·00	1·66
$Sr_6La_4(PO_4)_2(SiO_4)_4O$	5·99	4·00	1·99	4·01	1·66

3.2 *X-ray diffraction*

The powder X-ray diffraction patterns of the samples are shown in figure 1. All the peaks of each pattern matched well with the JCPDS pattern 44–654 indicating that the powders were single apatite phase. The lattice parameters are given in table 1. Those of the unsubstituted sample were in good agreement with the reported values.[29] The substitution induced an increase of α parameter and a decrease of *c* one, this opposite evolution was related on one hand to the size of substitutes, and on the other hand to the presence of vacancies in the channel.[30]

The structural refinement was performed using the FULLPROF program.[31] The previously obtained parameters[30] with the atomic coordinates of $Sr_{10}(PO_4)_6F_2$ were taken as preliminary data for the structural refinement of the unsubstituted compound. Then, the structural parameters of the substituted samples were refined using the data of $Sr_{10}(PO_4)_6O$ that were determined earlier. The background determination was performed with a five order polynomial. The pseudo-Voigt function was used to fit the experimental peak profiles. The refined factors were: The scale factor, the zero shift of the diffraction, the lattice constants, the full width at half maximum, the preferred orientation, the atomic parameters, the occupancy factors and the isotropic atomic displacement parameters. The refinement of the sites occupation was carried out with a distribution of La atoms over the two sites with the unique constraint of the chemical composition. The occupancy factors of O, P/Si were assumed to be constant.

The final R factors are given in table 1. The atomic coordinates and displacement parameters are summarized in table 3. The observed and calculated X-ray diffraction profiles as well as their difference are presented in figure 1. It should be noted that when the O(4) was placed in the special 2a position (0 0 1/4), its isotropic atomic displacement parameters were B = –1·07(3), –0·71(3) and –0·064(6) for $Sr_{10}(PO_4)_6O$, $Sr_8La_2(PO_4)_4(SiO_4)_2O$ and $Sr_6La_4(PO_4)_2(SiO_4)_4O$, respectively. These values seem to be unreasonable. This may be due to heavier atoms or some other problems. But, when this oxygen was allowed to move along this axis, i.e. located at the 4e position (0, 0, z), its isotropic atomic displacement parameters were refined to more reasonable values B = 0·89(3), 1·65(5) and 1·35(5), respectively. However, the values of R factors remained unchanged. For $Sr_{10}(PO_4)_6O$, O(4) was at the level $z = 0{\cdot}326(4)$. After inserting La^{3+} and SiO_4^{4-} into the oxyapatite framework, the O(4) shifted regularly towards the centre of the triangle formed by M(2)-

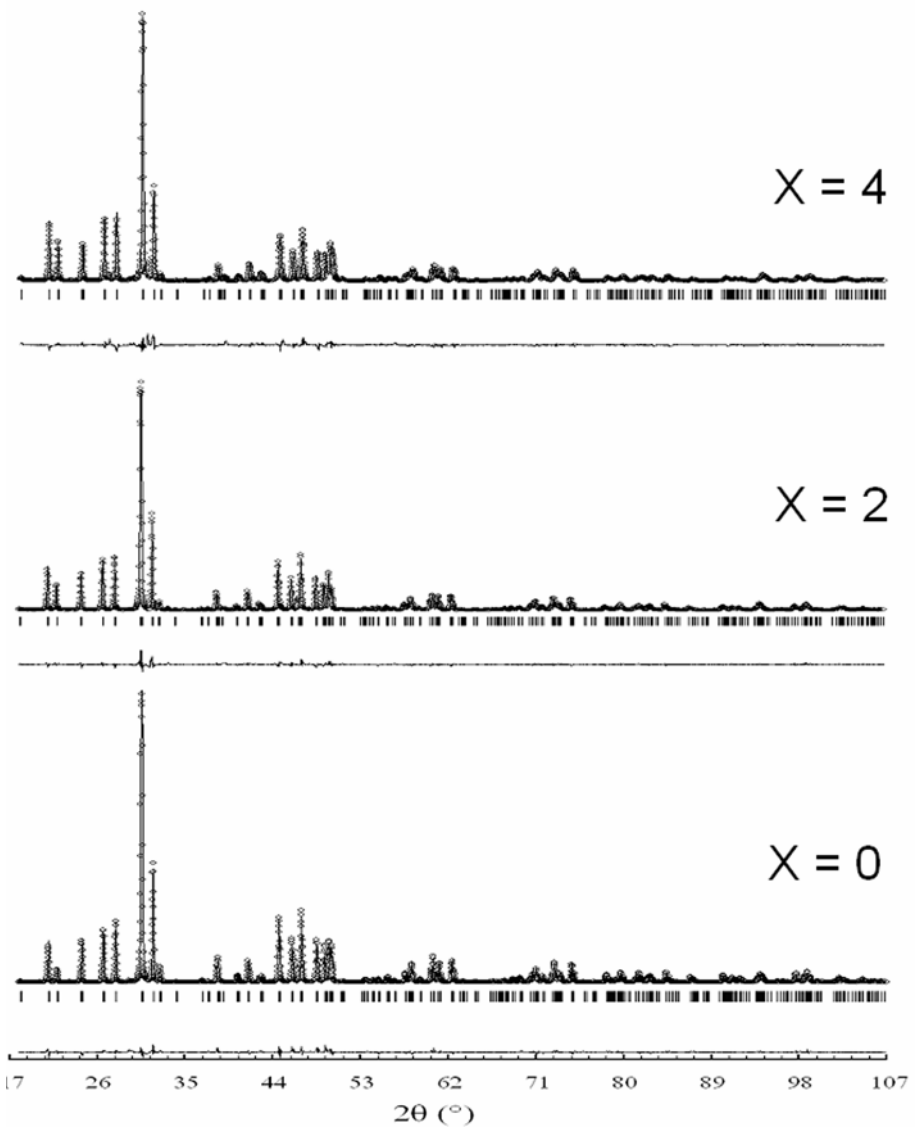

Figure 1. Experimental and calculated X-ray diffraction patterns, and their difference of $Sr_{10}(PO_4)_6O$, $Sr_8La_2(PO_4)_4(SiO_4)_2O$ and $Sr_6La_4(PO_4)_2(SiO_4)_4O$.

atoms ($z = 1/4$), at 0·323(3) and 0·293(7) for $Sr_8La_2(PO_4)_4(SiO_4)_2O$ and $Sr_6La_4(PO_4)_2(SiO_4)_4O$, respectively, while, for the corresponding fluorbritholites, the fluoride anion (F^-) shifted in the opposite way.[26] It is worth noticing that both solid solutions differ only by their monovalent anion, Y^-.

Previous studies indicated that in phosphate apatites, the Ln^{3+} ions occupy exclusively the (6 h) sites,[32,33] whereas when silicate groups are incorporated into the apatite structure, they are distributed over the two sites, with a marked preference for the (6 h) sites.[32] Preparing Ca–Nd–phosphosilicate, Carpena *et al* observed that the localization of Nd^{3+} ions in the cationic sites depended on operating conditions, but always with a preference for the (6 h) sites.[12] Preferential localization of Ln^{3+} ions in the (6 h) sites was essentially attributed to the formation of a strong bond between these cations and the anion located in the channel.[33] The refinements of the sites occupation were carried out with a statistical distribution of La^{3+} between the two sites taking as a constraint the chemical compoition of the compounds and the fact that both sites were fully and complementarily occupied by Sr^{2+} and La^{3+} ions. The occupancy factors of O and P/Si were assumed to be constant. The obtained results showed that the La^{3+} ions occupied preferentially the (6 h) sites (table 2). The rare earth element sites

Table 3. Atomic coordinates, occupancy factors and thermal parameters after Rietveld refinement of $Sr_{10-x}La_x(PO_4)_{6-x}(SiO_4)_xO$ samples.

Apatite	Atom	Wyckoff site	*x*	*y*	*z*	Site occupancy factor	Beq[Å^2]
$Sr_{10}(PO_4)_6O$	Sr(I)	4f	0·3333	0·6667	0·0006(3)	1	1·13(2)
	Sr(II)	6h	0·0145(1)	0·2587(1)	0·250	1	1·08(2)
	P	6h	0·3996(3)	0·3660(4)	0·250	1	1·00(7)
	O1	6h	0·3358(8)	0·4775(9)	0·250	1	1·23(17)
	O2	6h	0·5813(8)	0·4584(8)	0·250	1	0·78(16)
	O3	12i	0·3453(6)	0·2636(5)	0·075(6)	1	1·52(13)
	O4	4e	0·000	0·000	0·326(4)	0·25	0·89(3)
$Sr_8La_2(PO_4)_4(SiO_4)_2O$	Sr(I)	4f	0·333	0·666	0·0013(5)	0·976(2)	1·26(5)
	La(I)	4f	0·333	0·666	0·0013(5)	0·024(3)	1·26(5)
	Sr(II)	6h	0·0133(2)	0·250(2)	0·250	0·687(3)	1·55(3)
	La(II)	6h	0·0133(2)	0·250(2)	0·250	0·313(5)	1·55(3)
	P/Si	6h	0·3963(5)	0·3674(5)	0·250	1	0·94(11)
	O1	6h	0·3288(11)	0·4773(13)	0·250	1	1·86(3)
	O2	6h	0·5820(11)	0·4603(12)	0·250	1	1·17(3)
	O3	12i	0·3482(7)	0·2655(8)	0·0719(8)	1	1·54(2)
	O4	4e	0·000	0·000	0·3231(3)	0·25	1·65(5)
$Sr_6La_4(PO_4)_2(SiO_4)_4O$	Sr(I)	4f	0·333	0·666	0·0016(6)	0·739(7)	1·16(6)
	La(I)	4f	0·333	0·666	0·0016(6)	0·261(4)	1·16(6)
	Sr(II)	6h	0·0136(3)	0·2525(2)	0·250	0·508(3)	1·50(4)
	La(II)	6h	0·0136(3)	0·2525(2)	0·250	0·492(5)	1·50(4)
	P/Si	6h	0·3910(7)	0·3681(8)	0·250	1	0·63(8)
	O1	6h	0·3223(5)	0·4813(7)	0·250	1	1·68(4)
	O2	6h	0·5938(6)	0·4713(9)	0·250	1	1·02(2)
	O3	12i	0·3485(4)	0·2683(4)	0·0680(6)	1	2·58(3)
	O4	4e	0·000	0·000	0·293(7)	0·25	1·35(5)

occupancy ratios [La(1)/La(2)] are 0·051 and 0·353, respectively. For the fluorbritholites,[26] these values were 0·182 and 0·355, respectively. While in the statistical distribution, the occupancy ratio [La(1)/La(2)] has a value of 0·666. As it was observed, La^{3+} ions occupied preferentially the M(2) sites in both solid solutions. The tendency of La^{3+} to occupy the M(2) sites was greater for the smallest content, and it was even more marked for the oxybritholites. Nevertheless, regarding the values of the ratio La(1)/La(2) for $x = 4$, the shift of O(4) and F in opposite way along the six-fold axis can not be explained by a difference in the distriution of La over the two sites.

Selective interatomic distances and angles, together with distortion indices, are presented in table 4. After incorporation of SiO_4 into the apatite structure, the mean P/Si–O values were 1·548 and 1·598 Å for $x = 2$ and 4, respectively. They are longer than the mean P–O value (1·530 Å) in the unsubstituted compound agreeing with the P–O distance (1·51 Å) and Si-O one (1·62 Å) in PO_4 and SiO_4 tetrahedrons,[34] respectively. The mean angles O–P/Si–O did not vary significantly: 109·46, 109·43 and 109·33°, for $x = 0$, 2 and 4, respectively. However, the examination of the different angle values for the three compounds showed that the tetrahedrons were slightly deformed; the standard deviation of these angles varies from 1·64 to 4·26°. With the increase of *x*, the Sr/La(1)–O(2) distance slightly increased, while the other Sr/La(1)–O distances decreased significantly. Concerning the Sr/La(2)–O bond length, we noted that the Sr/La(2)–O(3) distance was longer than the Sr(2)–O(3) one, whereas all the other Sr/La(2)–O bond lengths were smaller. Thus, after substitution, the oxygen atoms were rearranged around the La atom to accommodate the weak constraints due to the presence of the silicates.[35] In addition, the Sr/La(2)–O(4) distance decreased. This latter decrease might be related to two concomitant effects: (i) the ionic radii difference; when larger Sr^{2+} ions (coord. 7: $r = 1{\cdot}35$ Å) occupy the (6 h) sites, the space at the center of the triangle is reduced and the oxide ion must accommodate outside, with the incorporation of La^{3+} ions (coord. 7: $r_{La^{3+}} = 1{\cdot}24$ Å), this space widened, and the O(4)

Table 4. Selected inter atomic distances (Å), angles (°) and distortion indices for $Sr_{10-x}La_x(PO_4)_{6-x}(SiO_4)_xO$ compounds.

	$Sr_{10}(PO_4)_6O$	$Sr_8La_2(PO_4)_4(SiO_4)_2O$	$Sr_6La_4(PO_4)_2(SiO_4)_4O$
(P, Si)–(O1)	1·501(1)	1·513(1)	1·549(1)
(P, Si)–(O2)	1·537(1)	1·569(2)	1·710(1)
(P, Si)–(O3)(× 2)	1·541(1)	1·555(1)	1·568(2)
⟨(P, Si)–O⟩	1·530	1·548	1·598
(O1)–(P, Si)–(O2)	110·48(9)	112·15(9)	111·27(17)
(O1)–(P, Si)–(O3)(× 2)	109·73(6)	110·70(6)	112·10(12)
(O2)–(P, Si)–(O3)(× 2)	107·62(6)	105·16(9)	102·88(12)
(O3)–(P, Si)–(O3)	111·59(4)	112·73(6)	114·78(10)
⟨O–(P, Si)–O⟩	109·46	109·43	109·33
(Sr1, La1)–O(1)(× 3)	2·600(3)	2·569(2)	2·513(1)
(Sr1, La1)–O(2)(× 3)	2·558(1)	2·564(1)	2·567(1)
(Sr1, La1)–O(3)(× 3)	2·913(2)	2·884(1)	2·878(1)
⟨(Sr1, La1)–O⟩	2·690	2·672	2·653
(Sr2, La2)–O(1)	2·777(1)	2·737(2)	2·702(1)
(Sr2, La2)–O(2)	2·517(1)	2·514(1)	2·444(1)
(Sr2, La2)–O(3)(× 2)	2·491(2)	2·477(2)	2·451(2)
(Sr2, La2)–O(3)(× 2)	2·702(1)	2·708(1)	2·735(3)
⟨(Sr2, La2)–O⟩	2·612	2·603	2·586
(Sr2, La)–O(4)	2·521(4)	2·491(4)	2·416(3)
DI ((P, Si)–O)	0·0094	0·0113	0·0345
DI (O–(P, Si)–O)	0·0082	0·018	0·0393

position shifted towards the center of the triangle leading to a short Sr/La(2)–O(4) distance; (ii) the charge of La^{3+}, which is more important than that of Sr^{2+}. Both effects led to the formation of a strong bond, which strengthens when more La occupy these positions.

According to the works of Ardhaoui *et al*,[21–23] the thermodynamic stability of the Ca–La–oxyabritholites increased and that of Ca–La–fluorbritholites decreased as the substitution of (La^{3+}; SiO_4^{4-}) for (Ca^{2+}; PO_4^{3-}) rose. These authors suggested that the increase of the stability of the oxybritholites would be related to the difference between the energies of the bonds Si–O (799 kJ mol^{-1}) and La–O (799 kJ mol^{-1}), and those of P–O (599 kJ mol^{-1}) and Ca–O (402 kJ mol^{-1}).[36] However, this difference in the energies bonds, as they mentioned, could not explain the decrease of the stability of Ca–La–fluorbritholites, especially, as the bond energies of Ca–F and La–F are (527 kJ mol^{-1}) and (598 kJ mol^{-1}),[36] respectively. In this issue, if we assumed that the same behaviour occurred for the analog Sr–La–britholites, and as these two kinds of solid solutions differ only by their monovalent anion, Y^-, it would seem that their difference in stability as the substitution increased would be related to the nature of this anion. As it was shown previously, for Sr–La–oxybritholites, the progressive shift of the free oxygen O(4) towards the centre of the triangles formed by the metal–atoms in the (6 h) positions strengthens the Sr/La(2)–O(4) bond,[33,37] which should confer a greater stability to the apatite structure with the increase of the substitution. However, the shift of the F^- position outside the centre of the triangle should weaken Sr/La(2)–F bond explaining, consequently, the decrease in the thermodynamic stability of these compounds.

3.3 *Raman spectra*

The FT–IR spectra of the synthesized materials presented the absorption bands relative to PO_4 and SiO_4 groups in an apatitic environment.[30]

The Raman spectra of the samples are given in figure 2. The band positions are summarized in table 5, with assignments according to the literature.[38–42] External modes corresponding to the liberational modes of PO_4 and SiO_4 groups, and translation ones of PO_4^{3-}, SiO_4^{4-}, Sr^{2+} and La^{3+} ions were revealed in the frequencies range 100–300 cm^{-1} (figure 2a), while, the bands associated to the vibration modes of both tetrahedrons are shown in figure 2b. The PO_4 group was revealed by the band of a significant intensity around 950 cm^{-1} associated to the

Table 5. Assignments of the Raman bands for $Sr_{10-x}La_x(PO_4)_{6-x}(SiO_4)_xO$ samples.

$Sr_{10}(PO_4)_6O$	$Sr_8La_2(PO_4)_4(SiO_4)_2O$	$Sr_6La_4(PO_4)_2(SiO_4)_4O$	Assignment (cm^{-1})
141	149	–	$T(PO_4^{3-})$
169	169	–	$R(PO_4^{3-})$
–	–	159	La^{3+}
193	190	188	Sr^{2+}
–	–	210	$T'(SiO_4)$ and $L(SiO_4)$
240	242	–	Sr^{2+}
–	277	266	La–O and $T'(SiO_4)$
951	949	952	$\nu_1(PO_4^{3-})$
441	442	–	$\nu_2(PO_4^{3-})$
417	419	–	
1075	1075	–	$\nu_3(PO_4^{3-})$
1050	1045	–	
1037	–	–	
1024	–	–	
997	999	–	
621	–	–	$Y_4(PO_4^{3-})$
580	593	–	
595	581	580	
572	574	573	
–	846	846	$\nu_1(SiO_4^{4-})$
–	393	394	$\nu_2(SiO_4^{4-})$
	383	380	
–	869	866	$\nu_3(SiO_4^{4-})$
–	516	518	$\nu_4(SiO_4^{4-})$
–	1218	1213	Fluorescence (La)
–	1358	1354	
–	1560	1554	
–	1680	1678	
–	1826	1813	

symmetric stretching modes (ν_1) and the weaker bands observed at frequencies higher than 990 cm^{-1} attributed to the asymmetric stretching modes (ν_3). Also, the bands appearing in both ranges 450–410 cm^{-1} and 630–570 cm^{-1} were assigned to the symmetric and asymmetric bending modes (ν_2 and ν_4) of PO_4, respectively. In addition to the bands of PO_4 groups, the spectra of the substituted samples ($x = 2$ and 4) contained the bands associated with SiO_4 groups. The bands observed around 846 and 866 cm^{-1} were assigned to the symmetric (ν_1) and asymmetric (ν_3) stretching modes, respectively. However, the bands relative to the symmetric bending modes (ν_2) were detected in the range of 380–400 cm^{-1} and the band appearing near 516 cm^{-1} corresponded to the asymmetric bending mode (ν_4). The bands between 1100 and 2000 cm^{-1} were due to the fluorescence emission of rare earth element[43] (figure 2c). The increase of the x value was accompanied by the decrease of the intensities of PO_4^{3-} bands and the rise of those of SiO_4^{4-}.

3.4 *NMR spectroscopy*

The ^{31}P MAS NMR spectra exhibited a single resonance peak at 3·97, 3·30 and 2·19 ppm for $Sr_{10}(PO_4)_6O$, $Sr_8La_2(PO_4)_4(SiO_4)_2O$ and $Sr_6La_4(PO_4)_2(SiO_4)_4O$, respectively, indicating only one crystallographic site for the phosphor.[30] The solid ^{29}Si MAS NMR spectra of $Sr_8La_2(PO_4)_4(SiO_4)_2O$ and $Sr_6La_4(PO_4)_2(SiO_4)_4O$ compounds are presented in figure 3. Both spectra showed also a single resonance peak at −75·68 and −77·68 ppm. This result related to Q^0 silicon species[44] is in agreement with those obtained on apatites prepared in the La–Si–O system.[45] It seems that P and Si occupied the same crystallographic site into the apatite structure.

4. Conclusion

Lanthanum-substituted strontium–oxyapatites with the formula of $Sr_{10-x}La_x(PO_4)_{6-x}(SiO_4)_xO$ where $x = 0$, 2 and 4 were prepared by the solid state

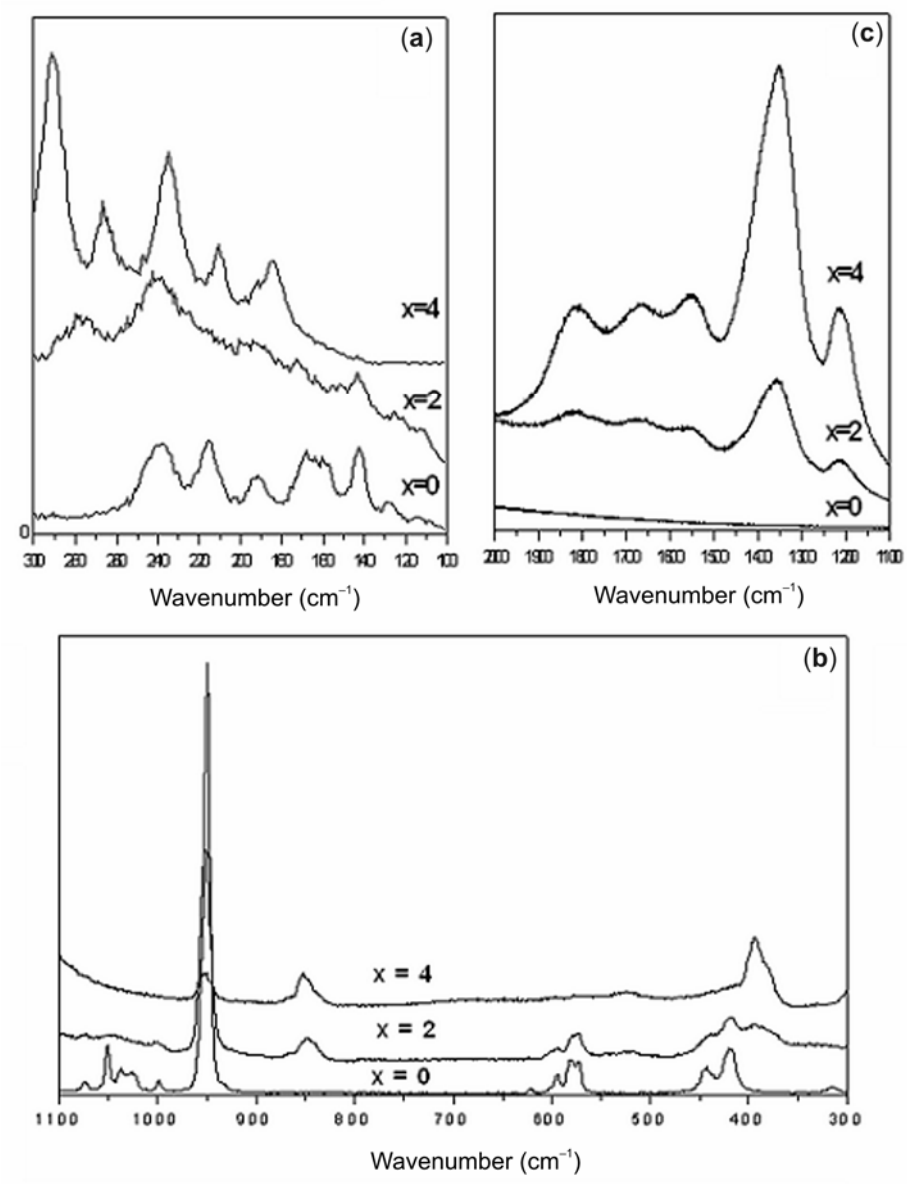

Figure 2. Raman spectra of $Sr_{10-x}La_x(PO_4)_{6-x}(SiO_4)_xO$ samples: Spectral ranges were in (**a**) 100–300 cm^{-1}, (**b**) 300–1100 cm^{-1} and (**c**) 1100–2000 cm^{-1}.

reaction at a temperature ranging between 1200 and 1400°C. The as-synthesized powders were characterized by X-ray diffraction, Raman spectroscopy and ^{29}Si MAS NMR. A structural investigation of these compositions was also performed using the Rietveld method. The findings showed that:

(i) The Lanthanum atoms preferentially occupied the (6 h) sites into the apatite structure.

(ii) When the substitution of (La^{3+}; SiO_4^{4-}) for (Ca^{2+}; PO_4^{3-}) increased, a progressive shift of the O(4) position towards the centre of the triangle formed by the M(2)-atoms occurred, which led to the formation of a strong bond between this oxygen and the atoms located in these sites. The formation of such a bond could contribute to a better stability of the apatite structure.

(iii) The increase of the substitution was accompanied by the decrease of the intensities of the Raman PO_4^{3-} bands and the rise of those of SiO_4^{4-} ones.

(iv) The Si atoms occupied one crystallographic site, as indicated by ^{29}Si MAS NMR, confirming the data determined by the Rietveld investigation.

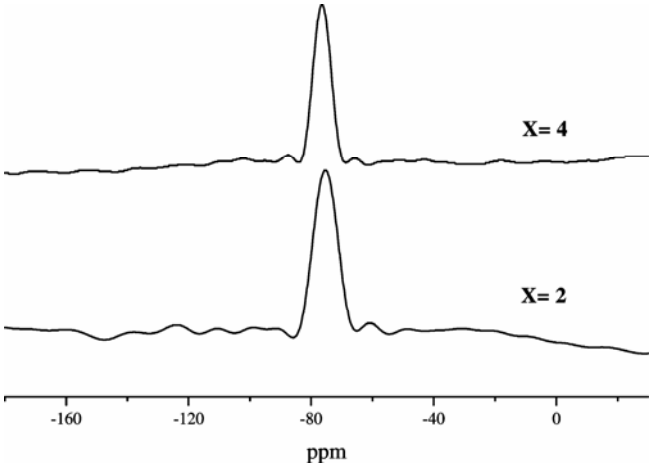

Figure 3. ^{29}Si MAS NMR spectra of $Sr_{10-x}La_x(PO_4)_{6-x}(SiO_4)_xO$ samples.

Acknowledgment

The authors would like to thank Mr Ridha Ben Abdlhafidh for his help in improving the manuscript with English corrections.

References

1. Elliot J C, Dykes E and Makie P E 1981 *Acta Cryst.* **B37** 435
2. Rey C 1995 *l'Actual. Chim. Dec.* 41
3. Sudarsanan K and Young R A 1969 *Acta Cryst.* **B25** 1534
4. Mayer I and Semadja A 1983 *J. Solid State Chem.* **46** 363
5. Aissa A, Badraoui B, Thouvenot R and Debbabi M 2004 *Eur. J. Inorg. Chem.* 3828
6. Badraoui B, Aissa A and Debbabi M 2007 *J. Phys. Chem. Solids* **68** 211
7. Kannan S, Rebelo A and Ferreira J M F 2006 *J. Inorg. Biochem.* **100** 1692
8. Ślósarczyk A, Paszkiewicz Z and Paluszkiewicz C 2005 *J. Mol. Struct.* **744** 657
9. El Feki H, Savariault J M, Ben Salah A and Jemal M 2000 *Solid State Sci.* **2** 577
10. Sprio S, Tampieri A, Landi E, Sandri M, Martorana S, Celotti G and Logroscino G 2008 *Mater. Sci. Eng.* **C28** 179
11. Boyer L, Carpéna J and Lacout J L 1997 *Solid State Ionics* **95** 121
12. Carpena J, Boyer L, Fialin M, Kienast J R and Lacout J L 2001 *C. R. Acad. Sci. Paris* **333** 373
13. Nakayama S, Aono H and Sadaoka Y 1995 *Chem. Lett.* **24** 431
14. Slater P R, Sansom J E H and Tolchard J R 2004 *Chem. Rec.* **4** 373
15. Sansom J E H, Richings D and Slater P R 2001 *Solid State Ionics* **139** 205
16. Bros R, Carpena J, Sere V and Beltritti A 1996 *Radiochim. Acta* **74** 277
17. Carpena J, Kienast J R, Ouzegane K and Jehanno C 1988 *Geol. Soc. Am. Bull.* **100** 1237
18. Carpena J 1998 in *Advances in fission track geochronology* (eds) P Van den Haute and de Corte (Dordrecht: Kluwer Academic Publishers) p. 91
19. Carpena J, Boyer L and Lacout J L 1998 *French Patent* **98** 11334
20. Meis C, Gale J D, Boyer L, Carpena J and Grosset J 2000 *J. Phys. Chem.* **A104** 5380
21. Ardhaoui K, Coulet M V, Ben Chérifa A, Carpena J, Rogez J and Jemal M 2006 *Thermochim. Acta* **444** 190
22. Ardhaoui K 2006 Synthèse, caractérisation et détermination des grandeurs thermochimiques de britholites à base de lanthane et néodyme Doctoral Thesis University of Tunis Tunisia
23. Ardhaoui K, Rogez J, Ben Chérifa A, Rogez J, Jemal M and Satre P 2006 *J. Therm. Anal. Calorim.* **86** 553
24. Fleet M E, Liu X and Pan Y 2000 *Am. Mineral.* **85** 1437
25. Fleet M E and Pan Y 1994 *J. Solid State Chem.* **111** 78
26. Boughzala K, Ben Salem E, Kooli F, Gravereau P and Bouzouita K 2008 *J. Rare Earth* **26** 483
27. Gee A and Deitz V R 1953 *Anal. Chem.* **25** 1320
28. Rietveld H M 1969 *J. Appl. Cryst.* **2** 65
29. JCPDS File no. 44–654
30. Boughzala K, Ben Salem E, Ben Chrifa A, Gaudin E and Bouzouita K 2007 *Mater. Res. Bull.* **42** 1221
31. Rodriguez-Carvajal 1990 In *Collected abstract of powder diffraction meeting*, vol. 127 Toulouse France
32. Fleet M E, Liu X and Pan Y 2000 *J. Solid. State Chem.* **149** 391
33. Schroeder L W and Mathew M 1978 *J. Solid State Chem.* **26** 383
34. Shannon R D 1976 *Acta Cryst.* **A32** 751
35. Louis-Achille V 1999 *Atomistic modelling study of lanthanides incorporation in the crystal lattice of an apatite* Doctoral Thesis University of Paris VI France
36. Lide D R 2004 *Handbook of chemistry and physics 85* Boca Raton (Fla.), London, New York: CRC Press 52
37. Piriou B, Fahini D, Dexpert-Ghys J, Taitai A and Lacout J L 1987 *J. Lumin.* **39** 97
38. Rodriguez-Reyna E, Fuentes A F, Maczka M, Hanuza J, Boulahya K and Amador U 2006 *J. Solid State Chem.* **179** 522
39. Benarafa L, Rghioui L, Nejjar R, Saidi Idrissi M, Knidriri M, Lorraux A and Wallart F 2005 *Spectrochim. Acta* **A61** 419
40. Khorari S, Cahay R, Rulmont A and Tarte P 1994 *Eur. J. Solid State Inorg. Chem.* **31** 921
41. Fowler B O 1974 *Inorg. Chem.* **13** 194
42. Neubauer J and Pollmann H 1995 *Neues. Jahrb. Mineral. Abh.* **168** 237
43. Aminzadeh A 1997 *Acta* **A49** 693
44. Engelhardt G and Michel D 1987 *High resolution solid-state NMR of silicates and zeolites* (Norwich: John Wiley)
45. Sansom J E H, Tolchard J R, Islam M S, Apperley D and Slater P R 2006 *J. Mater. Chem.* **16** 1410